

Transverse Single Spin Asymmetry in $p + p^\uparrow \rightarrow J/\psi + X$

Rohini M. Godbole

Centre for High Energy Physics, Indian Institute of Science, Bangalore, India.^{*}

Abhiram Kaushik

Centre for High Energy Physics, Indian Institute of Science, Bangalore, India.[†]

Anuradha Misra

Department of Physics, University of Mumbai, Mumbai, India.[‡]

Vaibhav Rawoot

Department of Physics, University of Mumbai, Mumbai, India.[§]

Bipin Sonawane

Department of Physics, University of Mumbai, Mumbai, India.[¶]

(Dated: June 10, 2022)

Abstract

We present predictions of transverse single spin asymmetry (TSSA) in $p + p^\uparrow \rightarrow J/\psi + X$ using the color evaporation model of charmonium production in a generalized parton model (GPM) framework. For this purpose, we have used best fit parameters for the gluon Sivers function (GSF) extracted from PHENIX data on TSSA in $p + p^\uparrow \rightarrow \pi^0 + X$ at midrapidity. We calculate asymmetry at $\sqrt{s} = 115$ GeV, 200 GeV and 500 GeV and compare the results at 200 GeV with PHENIX data on TSSA in the process $p + p^\uparrow \rightarrow J/\psi + X$. We also investigate the effect of the transverse momentum dependent (TMD) evolution of the densities involved, on the asymmetry.

^{*}Electronic address: rohini@chepr.iisc.ernet.in

[†]Electronic address: abhiramb@chepr.iisc.ernet.in

[‡]Electronic address: misra@physics.mu.ac.in

[§]Electronic address: vaibhavrawoot@gmail.com

[¶]Electronic address: bipin.sonawane@physics.mu.ac.in

I. INTRODUCTION

The role of intrinsic transverse momentum and spin distribution of partons inside the hadrons in explaining the azimuthal asymmetries arising in experiments involving polarized beams [1–3] has been a subject of keen interest during the past decade. Transverse Single Spin Asymmetries (TSSA’s), measured in meson production in hadronic collisions as well as in semi inclusive deep inelastic scattering (SIDIS) experiments, provide useful information towards understanding the transverse dynamics of partons inside the hadrons.

It is known for long [4] that the conventional QCD factorization with collinear parton distribution functions (PDFs) and fragmentation functions (FFs) is not sufficient to account for the single spin asymmetries (SSAs) observed experimentally. It is now well established that the SSAs observed in the hadroproduction of mesons and semi inclusive deep inelastic scattering (SIDIS) [5–8] can be explained in terms of orbital motion of quarks and gluons and the spin structure of nucleons. One of the two approaches towards building up a suitable framework involves generalization of the concept of collinear PDFs by including the transverse momentum and spin dependence of the partons into PDFs and FFs, which are then collectively referred to as TMDPDF’s. This approach known as TMD approach has been successful in explaining the existing data in some processes, for example in inclusive pion production in pp collisions [9] and Z production in pp and $p\bar{p}$ collisions [10]. In the Transverse Momentum Dependent factorization scheme [11–14], the hadronic cross-section is then expressed as a convolution of TMDPDFs, TMD FFs and partonic cross-section.

One of the interesting TMDPDFs, which has been a subject of a large number of studies is Sivers Function, which can be interpreted as the number density of unpolarized quarks or gluons inside a transversely polarized proton. Information on Sivers function can throw light on the 3-dimensional structure of nucleon and may also provide an estimate of the orbital angular momentum of quarks and gluons [15, 16]. It was introduced by Sivers in Ref. [17, 18] wherein a transverse momentum dependent PDF, now known as Sivers function, was introduced for the first time to account for the large asymmetries observed in pp^\uparrow scattering [17]. Quark Sivers function, which is usually coupled to reasonably well parametrized unpolarized fragmentation functions, has been one of the first TMDs extracted from data [15]. All the known information on quark Sivers function has been obtained from SIDIS data and $\gamma^* - N$ scattering in the centre of mass frame. Initial extractions of up and down quark

Sivers functions, from HERMES and COMPASS data, were obtained using parametrizations that did not take into account sea quarks [19, 20]. Later, magnitude of asymmetry for K^+ measured at HERMES indicated the possible contribution of sea quarks and fits were obtained taking into account contributions of sea quarks also [19]. Parametrizations of Sivers function for up and down quarks have been found to be in agreement with light-cone models [21] and a quark-diquark spectator model [22]. Extractions of quark Sivers function taking into account TMD evolution have also been obtained by performing a global fitting of all data on Sivers asymmetry in SIDIS from HERMES, COMPASS and Jefferson Lab [10] and based on these, predictions have been made for Sivers asymmetry in the DY process and W -boson production. Although there are many parametrizations available for quark Sivers function, not much information is available on gluon Sivers function (GSF). Some of processes which have been proposed for obtaining information about GSF are $pp^\uparrow \rightarrow \gamma + X$ [23], $pp^\uparrow \rightarrow D + X$ [24, 25], $pp^\uparrow \rightarrow \gamma + \text{jet} + X$ [23, 26], $pp^\uparrow \rightarrow \gamma^* + X \rightarrow \mu^+ \mu^- + X$ [23] and $pp^\uparrow \rightarrow \eta_{c/b} + X$ [27].

Heavy flavour production- both open and closed- are considered to be clean probes of GSF since heavy quarks are predominantly produced via gluon-gluon fusion and thus can be used to isolate gluon dynamics within hadrons [24, 28–30]. The possibility of getting information on the GSF by looking at D -meson production in polarized proton-proton scattering at RHIC has been discussed by Anselmino *et al.*, [24] using a saturated GSF. The first phenomenological study on the gluon Sivers function has recently been performed by D’Alesio, Murgia and Pisano [31], wherein the gluon Sivers function has been fitted to midrapidity data on transverse SSA in $pp \rightarrow \pi^0 + X$ measured by PHENIX collaboration at RHIC [1]. In our previous work, where we made predictions for TSSA in electroproduction of J/ψ , we had used parametrization of gluon Sivers function suggested by Boer and Vogelsang [32], in which the x -dependence of the GSF was modeled on that of the u and d quark Sivers functions. We will call these BV parameters in the following. In our recent work on TSSA in D-Meson production [33], we have used the directly fitted GSF parameters of Ref. [31] and have compared the estimates using these with the results obtained using BV parameters.

In this work, we present predictions for TSSA in the process $pp^\uparrow \rightarrow J/\psi + X$ using recent directly fitted parameters, which we will call DMP fits [31]. We compare these with predictions obtained using the BV parameters, which are based on experimentally fitted quark Sivers parameters [32]. We then compare our results with the recent measurements

of Sivers asymmetry at PHENIX experiment in J/ψ production [34]. Finally, to assess the effect of QCD evolution on asymmetry, we compare the predictions based on DGLAP and TMD evolution of PDFs and Sivers function. This comparison is performed using the BV parameters because fits of the GSF with TMD evolution taken into account are currently not available.

II. FORMALISM

A. TSSA in the process $p + p^\uparrow \rightarrow J/\psi + X$ using color evaporation model

We consider the transverse single spin asymmetry,

$$A_N = \frac{d\sigma^\uparrow - d\sigma^\downarrow}{d\sigma^\uparrow + d\sigma^\downarrow}. \quad (1)$$

for the process $p + p^\uparrow \rightarrow J/\psi + X$ using the colour evaporation model [35] of J/ψ production.

In the colour evaporation model, the total cross-section for the production of J/ψ at leading order (LO) is proportional to the rate of $c\bar{c}$ production integrated over the invariant mass-squared range $4m_c^2$ to $4m_D^2$, where m_c is the mass of the charm quark and m_D is the open charm threshold [36]:

$$\sigma^{p+p \rightarrow J/\psi + X} = F_{J/\psi} \int_{4m_c^2}^{4m_D^2} dM_{c\bar{c}}^2 \int dx_a dx_b \left[f_{g/p}(x_a) f_{g/p}(x_b) \frac{d\hat{\sigma}^{gg \rightarrow c\bar{c}}}{dM_{c\bar{c}}^2} + f_{q/p}(x_a) f_{\bar{q}/p}(x_b) \frac{d\hat{\sigma}^{q\bar{q} \rightarrow c\bar{c}}}{dM_{c\bar{c}}^2} \right] \quad (2)$$

Here, the CEM parameter $F_{J/\psi}$ is the fraction that gives the probability of J/ψ production below $D\bar{D}$ threshold.

In the following, we shall neglect the second term in Eq. 2 as the major contribution to heavy flavour production comes from gluon initiated partonic subprocesses. Assuming TMD factorization, we generalize the above expression to include TMDPDFs and express the cross section for the transversely polarized scattering process $p + p^\uparrow \rightarrow J/\psi + X$ as

$$\sigma^{p+p^\uparrow \rightarrow J/\psi + X} = F_{J/\psi} \int_{4m_c^2}^{4m_D^2} dM_{c\bar{c}}^2 \int dx_a d^2 \mathbf{k}_{\perp a} dx_b d^2 \mathbf{k}_{\perp b} f_{g/p}(x_a, \mathbf{k}_{\perp a}) f_{g/p^\uparrow}(x_b, \mathbf{k}_{\perp b}) \frac{d\hat{\sigma}^{gg \rightarrow c\bar{c}}}{dM_{c\bar{c}}^2} \quad (3)$$

where the gluon densities have been replaced by transverse momentum dependent gluon PDFs. In Eq. 3, $f_{g/p^\uparrow(\downarrow)}(x, \mathbf{k}_\perp)$ is the TMDPDF describing the distribution of gluons in the

proton that transversely polarized w.r.t the beam axis with the polarization being upwards (downwards) with respect to the production plane. For a general value of the transverse spin \mathbf{S}_\perp , it is parametrised in terms of the gluon Sivers function (GSF) $\Delta^N f_{g/p^\uparrow}$, as follows:

$$\begin{aligned} f_{g/p^\uparrow}(x, \mathbf{k}_\perp, \mathbf{S}_\perp; Q) &= f_{g/p}(x, k_\perp; Q) - f_{1T}^{\perp i}(x, k_\perp; Q) \frac{\epsilon_{ab} k_\perp^a S_\perp^b}{M_p} \\ &= f_{g/p}(x, k_\perp; Q) + \frac{1}{2} \Delta^N f_{g/p^\uparrow}(x, \mathbf{k}_\perp, \mathbf{S}_\perp; Q) \\ &= f_{g/p}(x, k_\perp; Q) + \frac{1}{2} \Delta^N f_{g/p^\uparrow}(x, k_\perp; Q) \frac{\epsilon_{ab} k_\perp^a S_\perp^b}{k_\perp}. \end{aligned} \quad (4)$$

Any non-zero TSSA in the process considered would primarily arise due to an azimuthal anisotropy in the distribution of gluon transverse momenta in the polarized parton. This anisotropy is parametrised by the gluon Sivers distribution.

Following Ref. [37] we can then write the numerator and denominator of Eq. 1 as,

$$\begin{aligned} \frac{d^3 \sigma^\uparrow}{dy d^2 \mathbf{q}_T} - \frac{d^3 \sigma^\downarrow}{dy d^2 \mathbf{q}_T} &= \frac{F_{J/\psi}}{s} \int [dM_{c\bar{c}}^2 d^2 \mathbf{k}_{\perp a} d^2 \mathbf{k}_{\perp b}] \Delta^N f_{g/p^\uparrow}(x_a, \mathbf{k}_{\perp a}) f_{g/p}(x_b, \mathbf{k}_{\perp b}) \\ &\quad \times \delta^2(\mathbf{k}_{\perp a} + \mathbf{k}_{\perp b} - \mathbf{q}_T) \hat{\sigma}_0^{gg \rightarrow c\bar{c}}(M_{c\bar{c}}^2) \end{aligned} \quad (5)$$

and

$$\begin{aligned} \frac{d^3 \sigma^\uparrow}{dy d^2 \mathbf{q}_T} + \frac{d^3 \sigma^\downarrow}{dy d^2 \mathbf{q}_T} &= \frac{2F_{J/\psi}}{s} \int [dM_{c\bar{c}}^2 d^2 \mathbf{k}_{\perp a} d^2 \mathbf{k}_{\perp b}] f_{g/p}(x_a, \mathbf{k}_{\perp a}) f_{g/p}(x_b, \mathbf{k}_{\perp b}) \\ &\quad \times \delta^2(\mathbf{k}_{\perp a} + \mathbf{k}_{\perp b} - \mathbf{q}_T) \hat{\sigma}_0^{gg \rightarrow c\bar{c}}(M_{c\bar{c}}^2), \end{aligned} \quad (6)$$

with,

$$x_{a,b} = \frac{M_{c\bar{c}}}{\sqrt{s}} e^{\pm y}. \quad (7)$$

Here, y and \mathbf{q}_T are the rapidity and transverse momentum of the J/ψ and we consider the plane of production of the J/ψ to be perpendicular to the proton spin \mathbf{S}_\perp . The partonic cross-section for production of a $c\bar{c}$ pair of mass M is given by [36]

$$\hat{\sigma}_0^{gg \rightarrow c\bar{c}}(M^2) = \frac{\pi \alpha_s^2}{3\hat{s}} \left[\left(1 + v + \frac{1}{16} v^2 \right) \ln \frac{1 + \sqrt{1 - v}}{1 - \sqrt{1 - v}} - \left(\frac{7}{4} + \frac{31}{16} v \right) \sqrt{1 - v} \right] \quad (8)$$

where $v = \frac{4m_c^2}{M^2}$.

B. Parametrization of the TMDs

For the predictions with the two DMP fits [31], we adopt the same functional forms for the TMDs using which they were extracted. We use the standard form for the unpolarized

TMDPDF with a factorized Gaussian k_\perp -dependence,

$$f_{i/p}(x, k_\perp; Q) = f_{i/p}(x, Q) \frac{1}{\pi \langle k_\perp^2 \rangle} e^{-k_\perp^2 / \langle k_\perp^2 \rangle} \quad (9)$$

with $\langle k_\perp^2 \rangle = 0.25 \text{ GeV}^2$. The Sivers function is parameterized as [38]

$$\Delta^N f_{i/p^\dagger}(x, k_\perp; Q) = 2\mathcal{N}_i(x) f_{i/p}(x, Q) h(k_\perp) \frac{e^{-k_\perp^2 / \langle k_\perp^2 \rangle}}{\pi \langle k_\perp^2 \rangle} \quad (10)$$

with,

$$\mathcal{N}_i(x) = N_i x^{\alpha_i} (1-x)^{\beta_i} \frac{(\alpha_i + \beta_i)^{\alpha_i + \beta_i}}{\alpha_i^{\alpha_i} \beta_i^{\beta_i}} \quad (11)$$

and

$$h(k_\perp) = \sqrt{2e} \frac{k_\perp}{M_1} e^{-k_\perp^2 / M_1^2}, \quad (12)$$

where \mathcal{N}_i , α_i , β_i and M_1 are all parameters determined by fits to data and e is Euler's number.

As mentioned in the introduction, the two DMP extractions of the GSF, namely SIDIS1 and SIDIS2 were obtained by fitting to data on TSSA in $p^\dagger p \rightarrow \pi^0 + X$ at RHIC with quark Sivers function (QSFs) extracted earlier from SIDIS data being used to account for the quark contribution to A_N . In obtaining the SIDIS1 fits, only the u and d flavour were taken into account, using the data on pion production from the HERMES experiment and positive hadron production from the COMPASS experiment. SIDIS2 parameters were obtained using flavour segregated data on pion and kaon production so here all three light flavours were taken into account. Furthermore, the QSFs used in the SIDIS1 fit were obtained with the set of fragmentation functions by Kretzer [39] and those of SIDIS2 were obtained with the set by de Florian, Sassot and Stratmann (DSS) [40]. The values of the parameters of the two fits are given in Table I. We give predictions for TSSA using these.

SIDIS1	$N_g = 0.65$	$\alpha_g = 2.8$	$\beta_g = 2.8$	$\rho = 0.687$	$\langle k_\perp^2 \rangle = 0.25 \text{ GeV}^2$
SIDIS2	$N_g = 0.05$	$\alpha_g = 0.8$	$\beta_g = 1.4$	$\rho = 0.576$	

TABLE I: DMP fit parameters. $\rho = M_1^2 / (\langle k_\perp^2 \rangle + M_1^2)$.

C. TMD Evolution

The energy evolution of a TMDPDF $F(x, k_\perp; Q)$ is best described through its Fourier transform into coordinate space which is given by

$$F(x, b; Q) = \int d^2 k_\perp e^{-i\vec{k}_\perp \cdot \vec{b}_\perp} F(x, k_\perp; Q). \quad (13)$$

The evolution of b -space TMDPDFs can then be written as,

$$F(x, b; Q_f) = F(x, b, Q_i) R_{pert}(Q_f, Q_i, b_*) R_{NP}(Q_f, b) \quad (14)$$

where R_{pert} is the perturbatively calculable part of the evolution kernel, R_{NP} is a nonperturbative Sudakov factor and $b_* = b/\sqrt{1 + (b/b_{\max})^2}$ is used to stitch together the perturbative part of the kernel which is valid for $b \ll b_{\max}$ with the nonperturbative part which is valid for large b . Following Ref. [10], we choose an initial scale $Q_i = c/b_*$ for TMD evolution. Here $c = 2e^{-\gamma_E}$ where γ_E is the Euler-Mascheroni constant.

Setting $Q_i = c/b_*$ and $Q_f = Q$, the perturbative part can be written as,

$$R_{pert} = \exp \left\{ - \int_{c/b_*}^Q \frac{d\mu}{\mu} \left(A \ln \frac{Q^2}{\mu^2} + B \right) \right\} \quad (15)$$

where $A = \Gamma_{\text{cusp}}$ and $B = \gamma^V$ are anomalous dimensions that can be expanded perturbatively. The expansion coefficients with the appropriate gluon anomalous dimensions at NLL are [10]

$$A^{(1)} = C_A \quad (16)$$

$$A^{(2)} = \frac{1}{2} C_F \left(C_A \left(\frac{67}{18} - \frac{\pi^2}{6} \right) - \frac{5}{9} C_A N_f \right) \quad (17)$$

$$B^{(1)} = -\frac{1}{2} \left(\frac{11}{3} C_A - \frac{2}{3} N_f \right) \quad (18)$$

The nonperturbative part of the evolution kernel, R_{NP} is

$$R_{NP} = \exp \left\{ -b^2 \left(g_1^{\text{TMD}} + \frac{g_2}{2} \ln \frac{Q}{Q_0} \right) \right\}, \quad (19)$$

where g_2 is a factor universal to all TMDPDFs and g_1 is TMDPDF specific and is proportional to the intrinsic transverse momentum width of the particular TMDPDF at the momentum scale Q_0 . Assuming a factorized Gaussian form at scale Q_0 , we have

$$g_1^{\text{unpol}} = \frac{\langle k_\perp^2 \rangle_{Q_0}}{4}, \quad g_1^{\text{Sivers}} = \frac{\langle k_{s\perp}^2 \rangle_{Q_0}}{4}, \quad (20)$$

Expanding the TMDPDF $F(x, b; Q)$ at the initial scale in terms of its corresponding collinear density at leading order (LO), for the unpolarized TMDPDF we get,

$$\begin{aligned} f_{i/p}(x, b; Q) &= f_{i/p}(x, c/b_*) \exp \left\{ - \int_{c/b^*}^Q \frac{d\mu}{\mu} \left(A \ln \frac{Q^2}{\mu^2} + B \right) \right\} \\ &\times \exp \left\{ -b^2 \left(g_1^{\text{unpol}} + \frac{g_2}{2} \ln \frac{Q}{Q_0} \right) \right\} \end{aligned} \quad (21)$$

In the case of the Sivers function, the evolution of its derivative in b -space can be written in the form of Eq. 14 leading to,

$$\begin{aligned} f_{1T}^{\prime \perp i}(x, b; Q) &= \frac{M_p b}{2} T_{i,F}(x, x, c/b_*) \exp \left\{ - \int_{c/b^*}^Q \frac{d\mu}{\mu} \left(A \ln \frac{Q^2}{\mu^2} + B \right) \right\} \\ &\times \exp \left\{ -b^2 \left(g_1^{\text{Sivers}} + \frac{g_2}{2} \ln \frac{Q}{Q_0} \right) \right\}, \end{aligned} \quad (22)$$

where $f_{1T}^{\prime \perp}(x, b; \mu) \equiv \frac{\partial f_{1T}^{\perp}}{\partial b}$. Here the Qiu-Sterman function for parton i , $T_{i,F}(x, x, \mu)$ is obtained when expanding $f_{1T}^{\prime \perp}(x, x, \mu)$ at LO and can be parametrized as

$$T_{i,F}(x, x, \mu) = \mathcal{N}_i(x) f_{i/p}(x, \mu) \quad (23)$$

with $\mathcal{N}_i(x)$ having the same form as in Eq. 11.

The expressions for the TMDs in k_{\perp} -space can be obtained by Fourier transforming the b -space expressions:

$$f_{i/p}(x, k_{\perp}; Q) = \frac{1}{2\pi} \int_0^{\infty} db b J_0(k_{\perp} b) f_{i/p}(x, b; Q) \quad (24)$$

$$f_{1T}^{\prime \perp i}(x, k_{\perp}; Q) = \frac{-1}{2\pi k_{\perp}} \int_0^{\infty} db b J_1(k_{\perp} b) f_{1T}^{\prime \perp i}(x, b; Q) \quad (25)$$

The above expression for the Sivers function is related to $\Delta^N f_{i/p}^{\prime \perp}(x, k_{\perp}; Q)$ through Eq. 4.

For the purpose of studying the effect of the transverse-momentum-dependent evolution of the densities on the asymmetry predictions, we need to use the BV models for the GSF since there are no available fits of the GSF that take into account TMD evolution. We therefore consider the following two models of the GSF wherein the x -dependent term $\mathcal{N}_g(x)$, is modeled on that of the quarks:

1. BV (A): $\mathcal{N}_g(x) = (\mathcal{N}_u(x) + \mathcal{N}_d(x))/2$
2. BV (B): $\mathcal{N}_g(x) = \mathcal{N}_d(x)$

where both $\mathcal{N}_u(x)$ and $\mathcal{N}_d(x)$ are of the form given in Eq. 11. These models were first used in Ref. [32] by Boer and Vogelsang and hence we will refer to these as the BV models.

For the predictions with TMD evolved densities using the above two models, we use the following set of parameters given in Ref. [10],

$N_u = 0.106$	$\alpha_u = 1.051$	$\beta_u = 4.857$	$\langle k_{\perp}^2 \rangle_{Q_0} = 0.38 \text{ GeV}^2$
$N_d = -0.163$	$\alpha_d = 1.552$	$\beta_d = 4.857$	$\langle k_{s\perp}^2 \rangle_{Q_0} = 0.282 \text{ GeV}^2$
$b_{\max} = 1.5 \text{ GeV}^{-1}$			$g_2 = 0.16 \text{ GeV}^2$

TABLE II: Parameters for TMD evolved densities from Ref. [10].

The predictions made with the TMD evolved densities using the BV models are compared with those obtained with DGLAP evolved densities using the same models with the following set of parameters given in [41]

$N_u = 0.4$	$\alpha_u = 0.35$	$\beta_u = 0.36$	$\langle k_{\perp}^2 \rangle = 0.25 \text{ GeV}^2$
$N_d = -0.97$	$\alpha_d = 0.44$	$\beta_d = 0.9$	$M_1^2 = 0.19$

TABLE III: Parameters for DGLAP evolved densities from [41]

III. RESULTS

In this section, we present predictions of transverse single spin asymmetry in $p + p^{\uparrow} \rightarrow J/\psi + X$, obtained using the DMP fits [31] and the BV models [32] of the GSF for three different centre of mass energies $\sqrt{s} = 115 \text{ GeV}$ (AFTER@LHC), 200 GeV (RHIC1) and 500 GeV (RHIC2). We present asymmetry predictions as a function of (i) the transverse momentum q_T , with the rapidity integrated over the allowed range ($|y| < 3.4$ for $\sqrt{s} = 115 \text{ GeV}$, $|y| < 3.8$ for $\sqrt{s} = 200 \text{ GeV}$ and $|y| < 4.8$ for $\sqrt{s} = 500 \text{ GeV}$) and (ii) the rapidity y , with the transverse momentum integrated in the range $0 < q_T < 1.4 \text{ GeV}$. For convenience we will refer these two as q_T -asymmetry and y -asymmetry respectively. We then compare the predictions obtained using the aforementioned fits and models, with measurements of TSSA in $p + p^{\uparrow} \rightarrow J/\psi + X$ at $\sqrt{s} = 200 \text{ GeV}$, performed by the PHENIX collaboration at RHIC [34]. These measurements were performed in the forward ($1.2 \leq y \leq 2.2$), backward ($-2.2 \leq y \leq -1.2$) and midrapidity ($-0.35 \leq y \leq 0.35$) regions with $0 \leq q_T \leq 1.4$.

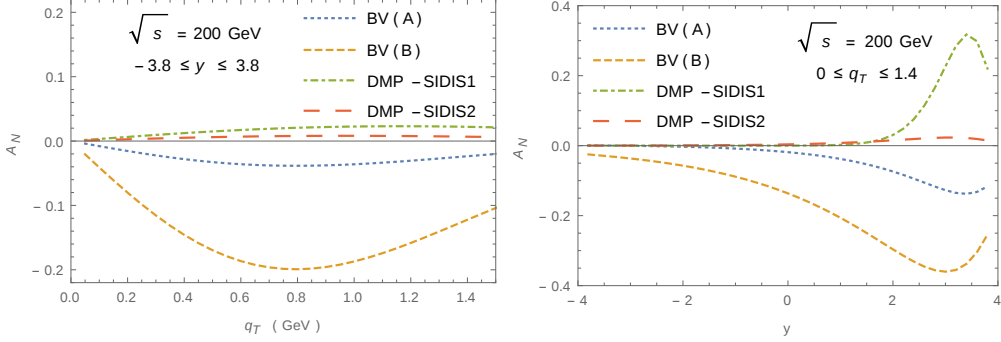


FIG. 1: Predictions of asymmetry in $p + p^{\dagger} \rightarrow J/\psi + X$ at RHIC1 ($\sqrt{s} = 200$ GeV) energy for all considered DGLAP evolved densities. Left panel and right panel show q_T -asymmetry (with $-3.8 \leq y \leq 3.8$) and y -asymmetry (with $0 \leq q_T \leq 1.4$) respectively.

In Figure 1, we show asymmetry predictions obtained using different sets of DGLAP evolved densities, i.e., the DMP fits and the BV models of the GSF at $\sqrt{s} = 200$ GeV.

In Figures 2 and 3, we present asymmetry predictions obtained with the DMP fits, SIDIS1 and SIDIS2, for all three centre of mass energies considered. In both cases, we find that the y -asymmetry scales with P_L/\sqrt{s} . This is because the collinear PDFs mostly cancel out between the numerator and the denominator and the y -dependence of the asymmetry is mostly determined by the remaining factor $\mathcal{N}_g(x)$, with x_a having a direct correspondence with y (c.f. Eq. 7). This cancellation is of course not absolute, as the integration over the invariant mass $M_{c\bar{c}}$ dilutes the correspondence of x_a with the rapidity and allows the collinear PDFs to affect the y -dependence, but we have verified that this effect is small. It must also be mentioned that the assumption that the k_{\perp} dependence of the TMD is factorized, helps this cancellation as the integrals over the transverse momenta of the partons do not depend on \sqrt{s} and simply produce an overall constant independent of both y and \sqrt{s} . We find peak asymmetry values of about 30% with SIDIS1 and 2% with SIDIS2, however in both cases, the rapidity at the asymmetry peak corresponds to the region $x_a > 0.3$ where the DMP fits do not constrain the GSF very well.

In case of the q_T -asymmetry, we find that the asymmetries decrease with increasing \sqrt{s} . However, the functional form of the q_T dependence remains the same upto an overall \sqrt{s} -dependent factor. This is also a reflection of the factorized k_T -dependence that we have assumed for the TMDPDFs. With SIDIS1, we find that peak asymmetry occurs at

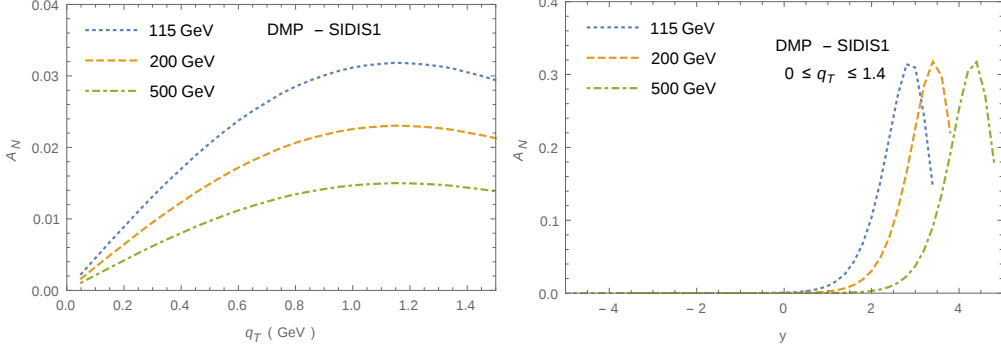


FIG. 2: Asymmetry predictions obtained using the DMP-SIDIS1 GSF [31] as a function of q_T (left) and y (right) for all three centre of mass values considered ($\sqrt{s} = 115$ GeV, 200 GeV, 500 GeV). Integration ranges for rapidity are $|y| < 3.4$ for $\sqrt{s} = 115$ GeV, $|y| < 3.8$ for $\sqrt{s} = 200$ GeV and $|y| < 4.8$ for $\sqrt{s} = 500$ GeV.

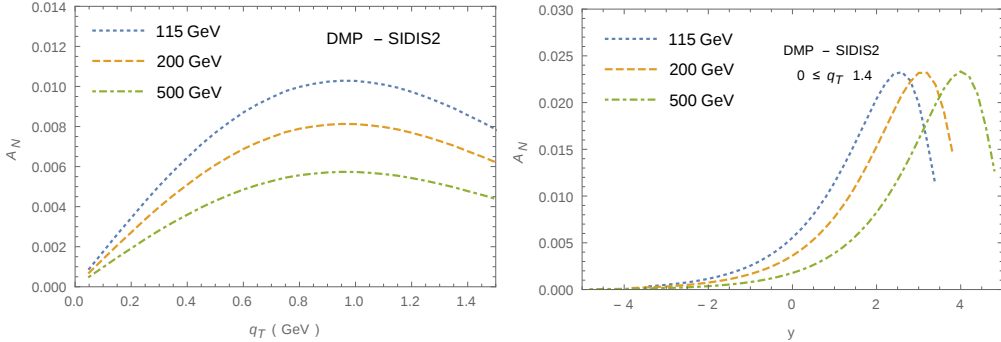


FIG. 3: Asymmetry predictions obtained using the DMP-SIDIS2 GSF [31] as a function of q_T (left) and y (right) for all three centre of mass values considered ($\sqrt{s} = 115$ GeV, 200 GeV, 500 GeV). Integration ranges for rapidity are $|y| < 3.4$ for $\sqrt{s} = 115$ GeV, $|y| < 3.8$ for $\sqrt{s} = 200$ GeV and $|y| < 4.8$ for $\sqrt{s} = 500$ GeV.

$q_T \sim 1.1\text{--}1.2$ GeV with peak asymmetry values of 3.2%, 2.3% and 1.5% for $\sqrt{s} = 115$, 200 and 500 GeV respectively, while for SIDIS2 we get substantially lower asymmetries with peak values of 1%, 0.8% and 0.55% for $\sqrt{s} = 115$, 200 and 500 GeV respectively at $q_T \sim 0.9\text{--}1.0$ GeV.

In Figure 4, we look at the effect of TMD evolution on the asymmetry predictions by comparing results obtained with DGLAP evolved densities with those obtained with TMD evolved densities. We do this using the BV (A) and BV (B) models of the GSF (c.f Section

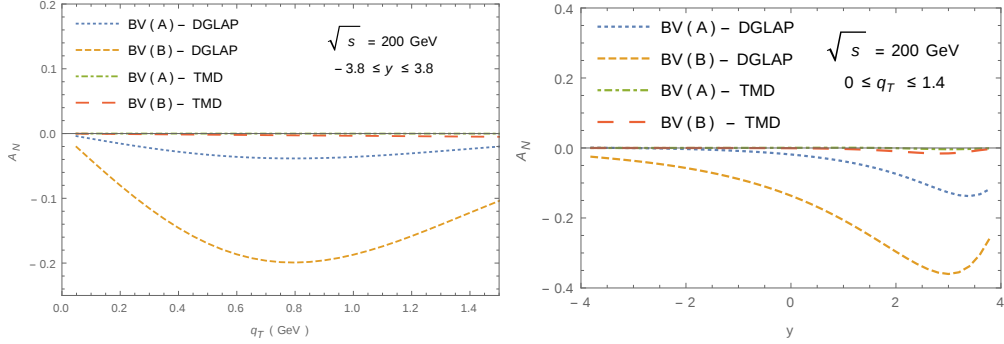


FIG. 4: Comparison of asymmetry predictions obtained using TMD evolved BV models [32] with those obtained using DGLAP evolved BV models. Left panel and right panel show q_T -asymmetry (with $-3.8 \leq y \leq 3.8$) and y -asymmetry (with $0 \leq q_T \leq 1.4$) respectively.

III C). We find that the inclusion of TMD evolution causes the asymmetry predictions to substantially decrease for both models. Furthermore the P_L/\sqrt{s} scaling of the y -asymmetry is also affected by TMD evolution as can be seen in Figure 5, where we show the asymmetries obtained with the TMD evolved BV (B) model, for all three c.o.m energies. While the peak of the asymmetry does shift to larger rapidities with increasing \sqrt{s} , the magnitude of the peak varies. This is due to the fact that the k_T -dependence of the TMDs is no more factorized, but is instead affected by the x -dependence of the collinear PDFs through the $c/b*$ prescription (c.f., Eq. 22, 23).

In Figures 6 and 7, we compare our predictions with the asymmetry measured at the PHENIX experiment [34]. In Figure 6, we compare the asymmetry predictions obtained using the DMP fits with the data and find that they lie well within the uncertainties. In the forward region both SIDIS1 and SIDIS2 give an asymmetry of about 2%. In Figure 7, we do the same using the DGLAP and TMD evolved BV models. With the DGLAP evolved models, BV (A) gives asymmetries which lie within the uncertainties except in the forward region, whereas BV (B) gives asymmetries well outside the uncertainties for all rapidity regions. However, the asymmetry predictions obtained with the TMD evolved BV models are substantially smaller than those given by DGLAP evolved BV models and are negligible in all rapidity regions.

In any case, the uncertainties in the data points are large and hence more data will be required to constrain the GSF in J/ψ production. The proposed fixed target experiment

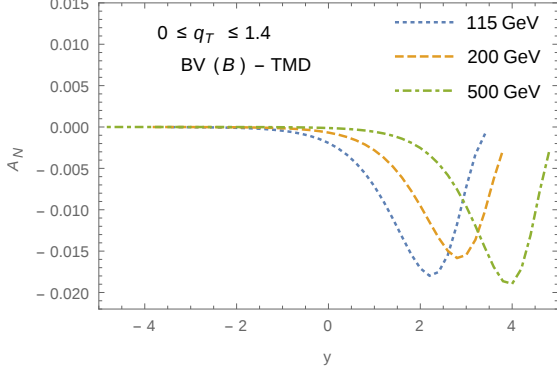


FIG. 5: Asymmetry predictions obtained using the TMD evolved BV (B) model of GSF [32] as a function of y for all three centre of mass values considered ($\sqrt{s} = 115$ GeV, 200 GeV, 500 GeV). Integration ranges for rapidity are $|y| < 3.4$ for $\sqrt{s} = 115$ GeV, $|y| < 3.8$ for $\sqrt{s} = 200$ GeV and $|y| < 4.8$ for $\sqrt{s} = 500$ GeV.

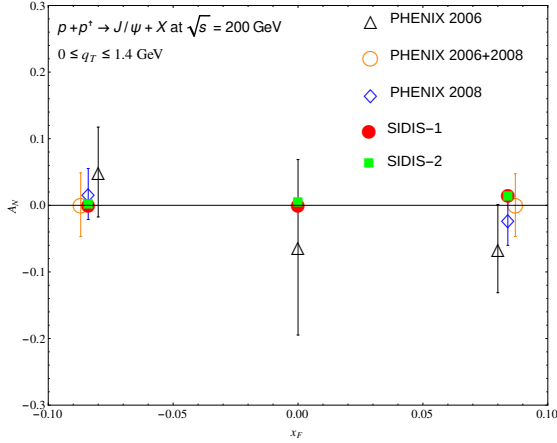


FIG. 6: Comparison of PHENIX measurements of TSSA in $p + p^+ \rightarrow J/\psi + X$ with predictions obtained using the DMP fits, SIDIS1 and SIDIS2 [31]. Asymmetry measurements are in the forward ($1.2 < y < 2.2$), backward ($-2.2 < y < -1.2$) and midrapidity ($|y| < 0.35$) regions with $0 \leq q_T \leq 1.4$.

AFTER@LHC would have a high enough luminosity to make precise measurements of the asymmetry [42]. Such a fixed target experiment would have a centre of mass energy $\sqrt{s} = 115$ GeV with an integrated luminosity of upto 20 fb^{-1} with one year of data taking. In such an experiment the pp centre of mass would be moving with respect to the lab frame with a rapidity $y_{\text{cms}} = 4.8$, allowing large x regions of the target to be probed with the coverage of the ALICE or LHCb detectors. A polarized target would therefore offer the possibility

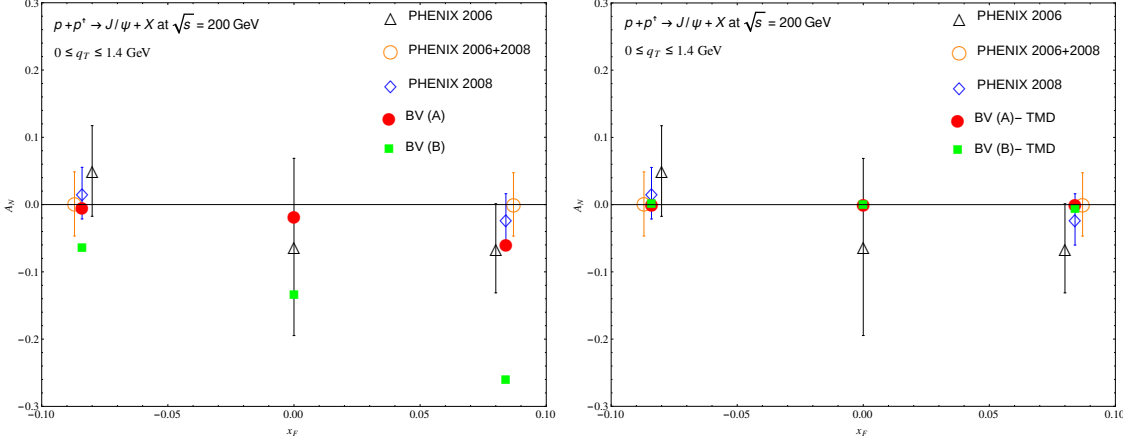


FIG. 7: Comparison of PHENIX measurements of TSSA in $p + p^\uparrow \rightarrow J/\psi + X$ with predictions obtained using BV models of the GSF [32]. Left panel shows comparison with DGLAP evolved BV models and right panel shows the same for TMD evolved BV models.

of probing large the x^\uparrow ($\gtrsim 0.3$) region where the DMP fits do not constrain the GSF. J/ψ production rates obtained with the leading order (LO) colour evaporation model (CEM) indicate that, with an integrated luminosity of 20 fb^{-1} , it should be possible to measure the asymmetry with permille precision in the low- q_T region with rapidity range $-3.0 \leq y \leq -2.0$ ($1.8 \leq y_{\text{cms}} \leq 2.8$). This roughly corresponds to the region $0.2 \lesssim x^\uparrow \lesssim 0.55$.

IV. CONCLUSIONS

In this paper, we have presented predictions of TSSA in $p + p^\uparrow \rightarrow J/\psi + X$ at the RHIC centre of mass energy $\sqrt{s} = 200 \text{ GeV}$, at which TSSA in J/ψ production has been measured by the PHENIX experiment. We have also presented predictions for $\sqrt{s} = 115 \text{ GeV}$, corresponding to the proposed polarized scattering experiment AFTER@LHC and $\sqrt{s} = 500 \text{ GeV}$, corresponding to the higher RHIC energy. Measurement of TSSA in J/ψ production at PHENIX experiment at RHIC has provided us an opportunity to compare our predictions with experimental results.

We have obtained predictions of TSSA with DGLAP as well as TMD evolved gluon densities. For the predictions with DGLAP evolved densities, we used recent extractions of GSF from TSSA measurements in $p^\uparrow p \rightarrow \pi^0 + X$, referred to here as the DMP parameter sets [31]. These extractions of GSF were obtained without taking into account TMD evolution. Hence

we have not used these parameters of GSF to assess the effect of TMD evolution. For this comparison of asymmetries calculated using DGLAP evolved and TMD evolved densities, we have used earlier models of the GSF which were in terms of u and d quark Sivers function and used in our previous work.

Our results show that the asymmetry obtained using BV parameterization is negative whereas asymmetry obtained using SIDIS parametrization is positive. This can be understood considering the fact that d quark Sivers function has negative sign. The q_T distribution of asymmetry we obtained with BV parametrization is large in magnitude as compared to asymmetry obtained with SIDIS parameterization. As far as the y distribution of asymmetry is concerned, the peak magnitudes of asymmetry are similar for all c.o.m energies, with the peak shifting towards larger rapidity values with increasing c.o.m energy. Comparison of our predictions of asymmetry with PHENIX measurement gives interesting results. When DGLAP evolved TMDs are used, our results with DMP-SIDIS1, DMP-SIDIS2 and BV (A) parametrizations are in agreement with the asymmetry data in forward, backward and midrapidity regions whereas the results obtained using BV (B) parametrization are not within experimental uncertainties of data points. However, when effect of TMD evolution is taken into account, results obtained using BV (B) parametrization also fall within experimental uncertainties. It may be worthwhile to obtain fits of GSF taking into account TMD evolution and compare predictions of asymmetry obtained using those with the predictions presented here.

As mentioned earlier, since the uncertainties in data points are large, more data will be needed to constrain the GSF. These studies to understand the GSF and resulting TSSA in pp^\uparrow are expected to play a crucial role in constraining the gluon spin dynamics.

V. ACKNOWLEDGEMENTS

A.M. and B.S. would like to thank DST, India for financial support under the project no.EMR/2014/0000486 and UGC-BSR under F.7-130/2007(BSR). A.M. would also like to thank the Theoretical Physics Department, CERN, Geneva, where part of this work was done, for their kind hospitality. R.M.G. wishes to acknowledge support from the Department of Science and Technology, India under Grant No. SR/S2/JCB-64/2007 under the J.C. Bose Fellowship scheme. A.K. would like to thank the Department of Physics, University of Mumbai, for their kind hospitality.

[1] A. Adare et al. (PHENIX), Phys. Rev. **D90**, 012006 (2014), 1312.1995.

[2] R. D. Klem, J. E. Bowers, H. W. Courant, H. Kagan, M. L. Marshak, E. A. Peterson, K. Rudnick, W. H. Dragoset, and J. B. Roberts, Phys. Rev. Lett. **36**, 929 (1976).

[3] J. Antille, L. Dick, L. Madansky, D. Perret-Gallix, M. Werlen, A. Gonidec, K. Kuroda, and P. Kyberd, Phys. Lett. **B94**, 523 (1980).

[4] G. L. Kane, J. Pumplin, and W. Repko, Phys. Rev. Lett. **41**, 1689 (1978).

[5] A. Airapetian et al. (HERMES), Phys. Rev. Lett. **103**, 152002 (2009), 0906.3918.

[6] M. Alekseev et al. (COMPASS), Phys. Lett. **B673**, 127 (2009), 0802.2160.

[7] C. Adolph et al. (COMPASS), Phys. Lett. **B717**, 383 (2012), 1205.5122.

[8] X. Qian et al. (Jefferson Lab Hall A), Phys. Rev. Lett. **107**, 072003 (2011), 1106.0363.

[9] U. D'Alesio and F. Murgia, Phys. Rev. **D70**, 074009 (2004), hep-ph/0408092.

[10] M. G. Echevarria, A. Idilbi, Z.-B. Kang, and I. Vitev, Phys. Rev. **D89**, 074013 (2014), 1401.5078.

[11] J. Collins, *Foundations of perturbative QCD* (Cambridge University Press, 2013), ISBN 9781107645257, 9781107645257, 9780521855334, 9781139097826, URL <http://www.cambridge.org/de/knowledge/isbn/item5756723>.

[12] X.-d. Ji, J.-P. Ma, and F. Yuan, Phys. Lett. **B597**, 299 (2004), hep-ph/0405085.

[13] X.-d. Ji, J.-p. Ma, and F. Yuan, Phys. Rev. **D71**, 034005 (2005), hep-ph/0404183.

[14] A. Bacchetta, D. Boer, M. Diehl, and P. J. Mulders, JHEP **08**, 023 (2008), 0803.0227.

[15] D. Boer et al. (2011), 1108.1713.

- [16] A. Bacchetta and M. Radici, Phys. Rev. Lett. **107**, 212001 (2011), 1107.5755.
- [17] D. W. Sivers, Phys. Rev. **D41**, 83 (1990).
- [18] D. W. Sivers, Phys. Rev. **D43**, 261 (1991).
- [19] M. Anselmino, M. Boglione, U. D'Alesio, S. Melis, F. Murgia, and A. Prokudin, J. Phys. Conf. Ser. **295**, 012062 (2011), 1012.3565.
- [20] M. Anselmino, M. Boglione, U. D'Alesio, A. Kotzinian, F. Murgia, and A. Prokudin, Phys. Rev. **D72**, 094007 (2005), [Erratum: Phys. Rev. D72, 099903 (2005)], hep-ph/0507181.
- [21] A. Bacchetta, F. Conti, and M. Radici, Phys. Rev. **D78**, 074010 (2008), 0807.0323.
- [22] L. P. Gamberg, G. R. Goldstein, and M. Schlegel, Phys. Rev. **D77**, 094016 (2008), 0708.0324.
- [23] I. Schmidt, J. Soffer, and J.-J. Yang, Phys. Lett. **B612**, 258 (2005), hep-ph/0503127.
- [24] M. Anselmino, M. Boglione, U. D'Alesio, E. Leader, and F. Murgia, Phys. Rev. **D70**, 074025 (2004), hep-ph/0407100.
- [25] Z.-B. Kang and J.-W. Qiu, Phys. Rev. **D78**, 034005 (2008), 0806.1970.
- [26] A. Bacchetta, C. Bomhof, U. D'Alesio, P. J. Mulders, and F. Murgia, Phys. Rev. Lett. **99**, 212002 (2007), hep-ph/0703153.
- [27] A. Schafer and J. Zhou, Phys. Rev. **D88**, 014008 (2013), 1302.4600.
- [28] F. Yuan, Phys. Rev. **D78**, 014024 (2008), 0801.4357.
- [29] S. J. Brodsky, D. S. Hwang, and I. Schmidt, Phys. Lett. **B530**, 99 (2002), hep-ph/0201296.
- [30] S. J. Brodsky, D. S. Hwang, and I. Schmidt, Nucl. Phys. **B642**, 344 (2002), hep-ph/0206259.
- [31] U. D'Alesio, F. Murgia, and C. Pisano, JHEP **09**, 119 (2015), 1506.03078.
- [32] D. Boer and W. Vogelsang, Phys. Rev. **D69**, 094025 (2004), hep-ph/0312320.
- [33] R. M. Godbole, A. Kaushik, and A. Misra, Phys. Rev. **D94**, 114022 (2016), 1606.01818.
- [34] A. Adare et al. (PHENIX), Phys. Rev. **D82**, 112008 (2010), [Erratum: Phys. Rev. D86, 099904 (2012)], 1009.4864.
- [35] M. B. Gay Ducati and C. Brenner Mariotto, Phys. Lett. **B464**, 286 (1999), hep-ph/9908407.
- [36] F. Halzen and S. Matsuda, Phys. Rev. **D17**, 1344 (1978).
- [37] R. M. Godbole, A. Misra, A. Mukherjee, and V. S. Rawoot, Phys. Rev. **D85**, 094013 (2012), 1201.1066.
- [38] M. Anselmino, M. Boglione, U. D'Alesio, A. Kotzinian, S. Melis, F. Murgia, A. Prokudin, and C. Turk, Eur. Phys. J. **A39**, 89 (2009), 0805.2677.
- [39] S. Kretzer, Phys. Rev. **D62**, 054001 (2000), hep-ph/0003177.

- [40] D. de Florian, R. Sassot, and M. Stratmann, Phys. Rev. **D75**, 114010 (2007), hep-ph/0703242.
- [41] M. Anselmino, M. Boglione, U. D'Alesio, S. Melis, F. Murgia, and A. Prokudin, in *19th International Workshop on Deep-Inelastic Scattering and Related Subjects (DIS 2011) Newport News, Virginia, April 11-15, 2011* (2011), 1107.4446, URL http://www1.jlab.org/U1/publications/view_pub.cfm?pub_id=11722.
- [42] J.-P. Lansberg et al., PoS **PSTP2015**, 042 (2016), 1602.06857.